Advanced Synthesis & Catalysis

DOI: 10.1002/adsc.201600010

Insights into the Molecular Recognition Process in Organocatalytic Chemoselective Monoacylation of 1,5-Pentanediol

Ayumi Imayoshi,[a] Masahiro Yamanaka,[b,*] Makoto Sato,[b] Keisuke Yoshida,[a] Takumi Furuta,[a] Yoshihiro Ueda,[a] and Takeo Kawabata[a,*]

[a] Institute for Chemical Research, Kyoto University, Uji, Kyoto 611-0011, Japan
E-mail: kawabata@scl.kyoto-u.ac.jp
[b] Department of Chemistry and Research Center for Smart Molecules, Faculty of Science, Rikkyo University, 3-34-1 Nishi-Ikebukuro, Toshima-ku, Tokyo 171-8501, Japan
E-mail: myamanak@rikkyo.ac.jp

Received: January 4, 2016; Revised: February 19, 2016; Published online: March 31, 2016

Supporting information for this article is available on the WWW under http://dx.doi.org/10.1002/adsc.201600010.

Abstract: Monoacylation of long-chain linear diols often encounters difficulties associated with unavoidable overacylation affording the diacylate. However, several C_1- and C_2-symmetrical pyrrolidinopyridine (PPY) catalysts were found to effectively promote the chemoselective monoacylation of 1,5-pentanediol. The effects of catalyst structure on the performance for the monoacylation were investigated. The amide carbonyl group(s) in the pyrrolidine ring in both C_1- and C_2-symmetrical catalysts was(were) suggested to play the key role in selective monoacylation. On the other hand, the indolyl NH group in the amide side chain of the catalysts was found to be critically important for further increasing the chemoselectivity of monoacylation only when the catalyst has a C_2-symmetrical structure. The effects of the catalyst structure on the chemoselective monoacylation were elucidated by DFT calculations, and the origin of the precise molecular recognition for 1,5-pentanediol by the catalysts and transition state (TS) stabilization effects by these functionalities were disclosed.

Keywords: acylation; diols; molecular recognition; organic catalysis; transition states

Introduction

Monoacylation of diols seems to be a simple molecular transformation, however, it is still known to be one of the difficult molecular transformations, because overacylation affording the diacylate is often unavoidable, especially for the acylation of long-chain linear diols. For example, acylation of 1,5-pentanediol (**1**) with the typical acylation catalyst, 4-dimethylaminopyridne (DMAP), afforded the monoacylate and the diacylate in a 1.7:1 ratio, even under the carefully controlled conditions at −60 °C (Table 1, entry 1).[1] To overcome the overacylation problem, the use of an excess amount of the diol substrate was often employed.[2] For example, acylation of 3.0–6.0 equivalents of **1** with an acid (acyl donor) in the presence of *N,N′*-dicyclohexylcarbodiimide (DCC) gave the monoacylate and the diacylate in a 3.5:1 ratio (Table 1, entry 2).[2c] Enzymatic acylation of **1** was reported to give the monoacylate selectively,[3] however, overacylation is again unavoidable (mono-/diacylate = 9.0).[3b] Against this background, we have developed a chiral pyrrolidinopyridine (PPY) catalyst **4** that enables the highly chemoselective monoacylation of linear diols. Acylation of **1** gave the monoacylate in a highly chemoselective manner in the presence of catalyst **4** (mono-/diacylate = 31:1, entry 4).[1] Highly chemoselective monoacylation of **1** with various acid anhydrides also proceeded in the presence of catalyst **4** (mono-/diacylate = 18 to > 50:1, entries 5–7).[1,4]

To elucidate the origin of the highly chemoselective monoacylation of 1,5-diol **1** promoted by catalyst **4**, kinetic study was performed.[1] A high relative rate $k_{1(\text{monoacylation})}/k_{2(\text{diacylation})}$ is supposed to be essential for selective monoacylation (Scheme 1a). As the measure of the relative rate of acylation (k_1/k_2), the relative rate of acylation between 1,5-diol **1** and monool-monoacylate **2′** was determined by competitive acylation between them. The relative rate for the acylation between **1** and **2′** was found to be 113 in the presence of catalyst **4**, whereas that in the presence of DMAP was 1.0 (Scheme 1b). The marked difference in the relative rates for acylation between **1** and **2′** was observed depending on the catalysts. Considering that the intrinsic reactivity of 1,5-diol **1** was assumed to be

Table 1. Mono- *vs.* diacylation of 1,5-pentanediol (**1**).

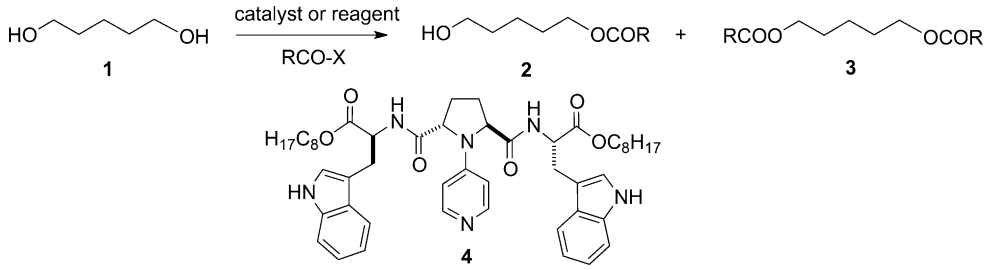

Entry	Conditions	R	**2** [%]	**3** [%]	**2**/**3**
1[a]	DMAP (5 mol%)/$(i\text{-PrCO})_2O$, −60 °C[b]	*i*-Pr	45	26	1.7
2[c]	DCC/$ArSO_2CH_2CO_2H$/THF[d]	$ArSO_2CH_2$	70	20	3.5
3[e]	Novozyme 871/$AcOCH{=}CH_2$/toluene	CH_3	81	9	9.0
4[a]	**4** (5 mol%)/$(i\text{-PrCO})_2O$ (1.1 equiv.), −60 °C[b]	*i*-Pr	92	3	31
5[a]	**4** (10 mol%)/$(AcCO)_2O$ (1.03 equiv.), −60 °C[b]	Ac	89	5	18
6[a]	**4** (10 mol%)/$(PhCO)_2O$ (1.03 equiv.), −60 °C[f]	Ph	64	≤1	>50
7[a]	**4** (10 mol%)/$(PhCH{=}CH_2CO)_2O$ (1.03 equiv.), −60 °C[g]	$PhCH{=}CH_2$	65	≤1	>50

[a] Data quoted from ref.[1]
[b] Run for 24 h.
[c] Data quoted from ref.[2c]
[d] Excess amounts (3.0–6.0 equivalents) of diol of **1** were used.
[e] Data quoted from ref.[3b]
[f] Run for 336 h.
[g] Run for 168 h.

equal to that of monoacylate **2′** based on the results from DMAP-catalyzed acylation, the observed strong preference for acylation of **1** over that of **2′** in the presence of catalyst **4** suggests that monoacylation of **1** may proceed in an accelerative manner by virtue of the precise molecular recognition of the substrate structure by catalyst **4**.

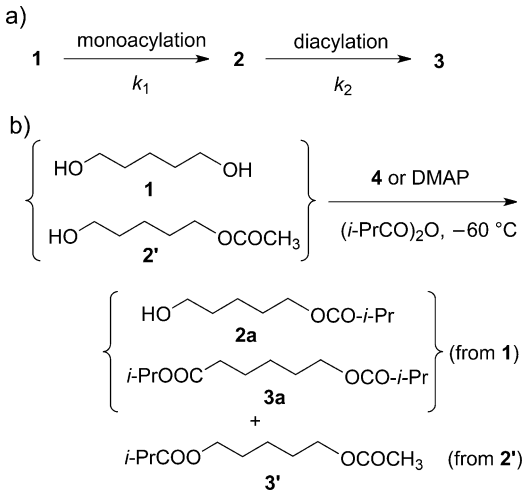

Entry	Catalyst	**2a**/**3a**/**3'**	$\frac{k\text{ (acylation of 1)}}{k\text{ (acylation of 2')}}$
1	**4**	91/8/4	113
2	DMAP	38/13/52	1.0

Scheme 1. a) Importance of a high k_1/k_2 ratio for chemoselective monoacylation for avoiding overacylation. b) Competitive acylation between 1,5-diol **1** and monool-monoacylate **2′**.

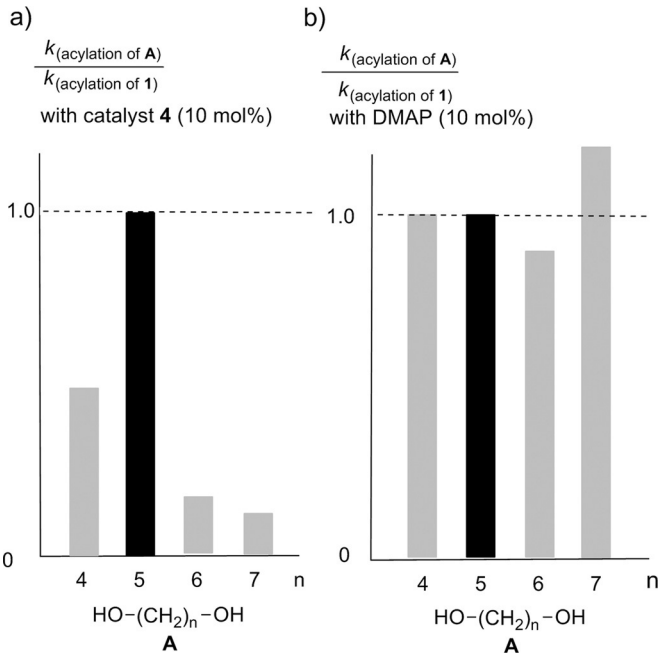

Figure 1. Relative rates of acylation of linear 1,*n*-diols ($n=4$–7) catalyzed by a) catalyst **4**, and b) DMAP. These data were created from the data reported in ref.[1], and standardized the rates of acylation based on the rate of acylation of 1,5-butanediol as 1.0 (shown as a black bar).

Preferential acylation of 1,5-diol **1** over other linear diols with different chain lengths was also observed in the presence of **4** (Figure 1a). The acylation of 1,5-diol **1** proceeded 2.0, 5.6, and 6.6 times faster than that of 1,4-butanediol, 1,6-hexanediol, and 1,7-heptanediol, respectively. On the other hand, acylation of these diols proceeded in almost equal rates with DMAP-catalyzed acylation (Figure 1b). Thus, catalyst **4** was found to be able to promote the chemoselective acylation of linear diols by discriminating their chain lengths. The observed phenomena in chemoselective acylation catalyzed by **4** obviously indicate that the molecular recognition process between catalyst **4** and the substrate diols would be involved. Here, we report our efforts to elucidate the molecular recognition process during the acylation of 1,5-pentanediol (**1**) catalyzed by **4** based on experimental results as well as theoretical studies.

Results and Discussion

We first examined the effects of the catalyst structure on the chemoselective monoacylation of **1**. Acylation of 1,5-diol **1** with 1.03 equivalents of isobutyric anhydride in the presence of chiral PPY catalysts **5**–**12** was examined (Table 2). The C_2-symmetrical catalysts **5** and **6**, each having amide side chains consisting of 1-methyl-L-tryptophan and L-2-naphlylalanine moiety, respectively, promoted the chemoselective monoacylation with much diminished selectivity (**2**/**3** = 8.0–8.5) and reactivity (57–63% conversion, entries 2 and 3), when compared with the acylation promoted by C_2-symmetrical catalyst **4** consisting of an L-tryptophan moiety (**2a**/**3a** = 27, 84% conversion, entry 1).[5] The marked difference in the properties of the catalysts in the chemoselective monoacylation suggests the critical importance of the indolyl NH group in catalyst **4** for the chemoselectivity. The effects of the C_2-symmetrical structure of the catalyst were next examined by employing the corresponding C_1-symmetrical catalysts, **7**–**9**. Chemoselective monoacylation took place in a similar selectivity (**2a**/**3a** = 10–15) and reactivity (32% conversion) in the presence of these catalysts, regardless of whether the indolyl NH group is involved in the catalyst structure or not (entries 4–6). It is worthy of note that the indolyl NH group is responsible for further increasing the selectivity and reactivity in the monoacylation of 1,5-diol **1** only when the PPY-catalyst has a C_2-symmetrical structure. Catalysts

Table 2. Effects of catalysts on chemoselectivity in the monoacylation of 1,5-diol **1**.

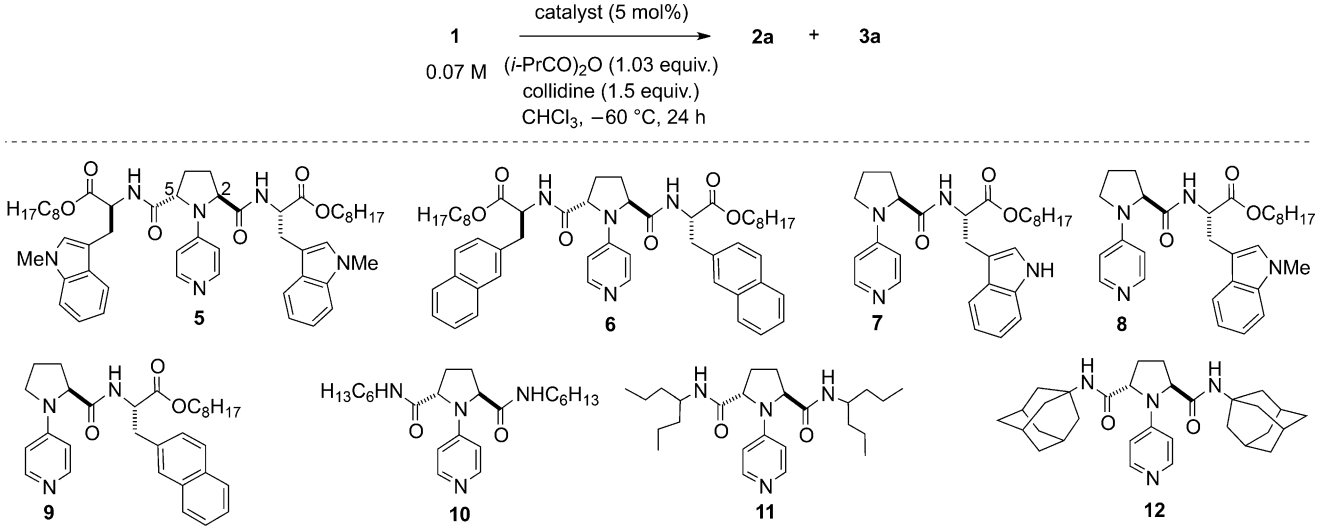

Entry	Catalyst	**2a** [%]	**3a** [%]	**2a**/**3a**	Recovery [%]
1	**4**	80	3	27	16
2	**5**	56	7	8.0	37
3	**6**	51	6	8.5	43
4	**7**	31	3	10	68
5	**8**	29	3	10	68
6	**9**	30	2	15	68
7[a,b]	**10**	76	5	15	16
8[a,b]	**11**	74	6	12	15
9[a,b]	**12**	67	7	10	23

[a] Data quoted from ref.[1]
[b] 1.1 equivalents of isobutyric anhydride were used.

10–12 possessing simple alkyl amide chains with different steric bulkiness also promoted the chemoselective monoacylation with comparable efficiency (**2a**/**3a** = 10–15), irrespective of the steric bulkiness of the amide side chains (entries 7–9). Thus, highly chemoselective monoacylation (**2a**/**3a** = 8.5–27) was observed throughout the catalysts examined, whose chemoselectivity was comparable or even higher than that reported for lipase-catalyzed monoacylation of **1** (**2a**/**3a** = 9.0: Table 1, entry 3).[3b] These results indicate that *the amide carbonyl group(s) at C-2 and/or C-5 of the pyrrolidine ring, common functionality in these PPY catalysts, seem(s) essential for the selective monoacylation, and the indolyl NH group in the amide side chain seems to be of critical importance for further increasing the chemoselectivity and reactivity only when the catalyst has a C_2-symmetrical structure.*

We next examined catalytic properties of **4–9** in acylation of 1,2-ethanediol (**13**) to compare them with those of 1,5-diol **1** (Table 3). The C_2-symmetrical PPY-catalysts **4–6** promoted the chemoselective monoacylation of **13** in high selectivities (**14**/**15** = 23–35, entries 1–3), regardless of whether the indolyl NH group is involved in the catalyst structure or not. Chemoselective monoacylation of 1,2-diol **13** with C_1-symmetrical catalysts **7–9** proceeded in slightly less, but still high, selectivities (**14**/**15** = 12–16, entries 4–6). The effect of the indolyl NH group in the catalysts did not significantly affect the chemoselectivity and reactivity of acylation of **13** promoted by both C_1- and C_2-symmetrical PPY- catalysts. In the case of acylation of 1,2-diol **13**, highly chemoselective acylation was observed throughout the C_1- and C_2-symmetrical catalysts. This could be ascribed mainly to the less intrinsic reactivity of monool-monoacylate **14** than that of 1,2-diol **13**, which seems to be in contrast to the case of acylation of 1,5-diol **1**.[6,7]

We then examined the catalytic properties of C_2-symmetrical PPY-catalysts **4–6** in the competitive acylation between 1,5-diol **1** and 1,2-diol **13** (Table 4).

Table 3. Effects of catalysts on chemoselectivity in the monoacylation of 1,2-diol **13**.

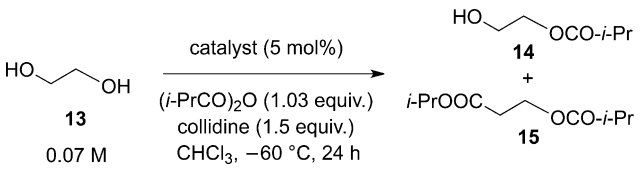

Entry	Catalyst	**14** [%]	**15** [%]	**14**/**15**	Recovery [%]
1	**4**	70	2	35	27
2	**5**	69	3	23	27
3	**6**	69	2	35	28
4	**7**	64	4	16	32
5	**8**	60	4	15	36
6	**9**	62	5	12	33

Table 4. Effects of catalysts on competitive acylation between 1,5-diol **1** and 1,2-diol **13**.

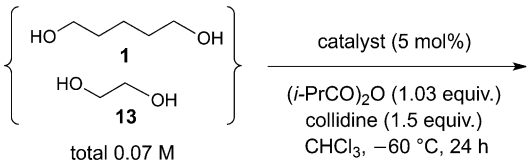

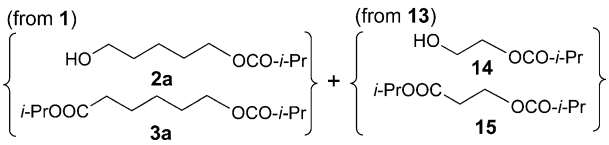

Entry	Catalyst	**2a**+**3a** [%]	**14**+**15** [%]	$\frac{k(\text{acylation of } \mathbf{1})}{k(\text{acylation of } \mathbf{13})}$ [a]
1	**4**	36	12	4.5
2	**5**	11	16	0.7
3	**6**	14	18	0.8

[a] Determined from the following equation.[b]

$$\frac{k(\text{acylation of } \mathbf{1})}{k(\text{acylation of } \mathbf{13})} = \frac{\ln\left[(1-\text{conversion})\left(1-\frac{|(\mathbf{14}+\mathbf{15})-(\mathbf{2a}+\mathbf{3a})|}{\{(\mathbf{14}+\mathbf{15})+(\mathbf{2a}+\mathbf{3a})\}}\right)\right]}{\ln\left[(1-\text{conversion})\left(1+\frac{|(\mathbf{14}+\mathbf{15})-(\mathbf{2a}+\mathbf{3a})|}{\{(\mathbf{14}+\mathbf{15})+(\mathbf{2a}+\mathbf{3a})\}}\right)\right]}$$

[b] The term $|(\mathbf{14}+\mathbf{15})-(\mathbf{2a}+\mathbf{3a})|$ indicates the absolute value of the difference between (**14**+**15**) and (**2a**+**3a**). Conversion was calculated based on the total amount of the two alcohols.

Relative rates of acylation ($k_{(\text{acylation of } \mathbf{1})}/k_{(\text{acylation of } \mathbf{13})}$) between **1** and **13** were determined by the competitive acylation between them in the presence of catalyst **4**, **5**, or **6**. Catalyst **4** with the indolyl NH group (NH_{indole}) promoted the acylation of 1,5-diol **1**, 4.5 times faster than that of 1,2-diol **13** (entry 1), whereas 1,2-diol **13** was acylated slightly faster than 1,5-diol **1** in the presence of catalysts **5** and **6** without the indolyl NH group (entries 2 and 3). The marked difference in the catalytic properties between catalysts **4–6** depending on the presence or the absence of the indolyl NH group indicates that *two indolyl NH groups arranged in a C_2-symmetrical fashion are essential for transition state (TS) stabilization resulting in accelerative monoacylation of 1,5-diol **1**.*

In the preliminary studies on chemoselective monoacylation of linear diols, we proposed a hypothetical transition state model for the acylation of **1** catalyzed by **4** (Figure 2).[1] This model may account for the preferential acylation of 1,5-diol **1** over the corresponding monool-monoacylate, **2a**, and also that over other linear diols with different chain lengths. However, the marked effect of the indolyl NH group in catalytic properties observed for preferential acylation of 1,5-diol **1** was not clear from this model. This background prompted us to further elucidate the mecha-

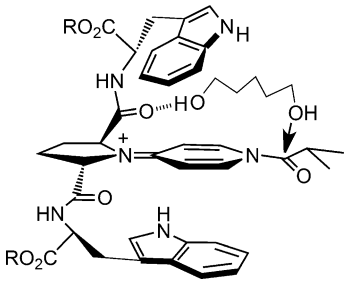

Figure 2. Previously proposed hypothetical transition state model without theoretical base for preferential monoacylation of 1,5-diol **1** catalyzed by **4**.

nistic aspects of the present organocatalytic chemoselective acylation based on computational studies.

Based on the experimental analysis of the substituent and the structural effects of catalyst **4**, DFT calculations were carried out (B3LYP/6-31G*)[8,9] using C_1- and C_2-symmetrical catalyst models (**cat1** and **cat2** in Scheme 2). To gain deep insights of the high chemoselectivity through TS stabilization, we investigated the

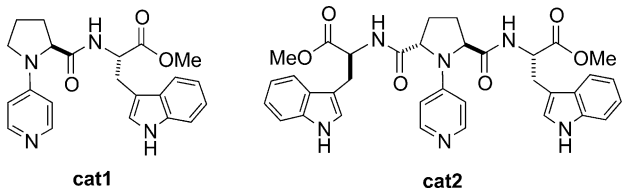

Scheme 2. Chemical models of PPY catalysts **7** (**cat1**) and **4** (**cat2**).

nucleophilic attack process in the monoacylation of 1,5-diol **1**. Preliminary screening of various coordination modes and conformational isomers of the catalyst and the substrates allowed us to identify the rational TS models of monoacylation and diacylation.[10]

We compared the relative Gibbs free energy differences between TSs of monoacylation and diacylation in each of the **cat1** and **cat2** systems (Figure 3). Monoacylation is energetically favored over diacylation in both systems. Whereas the diacylation TSs (**TSd**) are located at almost the same energy level, the monoacylation TSs (**TSm**) provides a significant impact on their stability. The Gibbs free energy difference between **TSm** and **TSd** increases from 3.1 kcal mol^{-1} in the **cat1** system to 6.0 kcal mol^{-1} in the **cat2** system by the significant stabilization of **TSm-cat2**. These computational results are qualitatively consistent with the experimental results.

The 3D structures and the relative Gibbs free energies of the most stable TSs in the **cat1**-catalyzed monoacylation (**TSm-cat1-1**) and diacylation (**TSd-cat1-1**) are shown in Figure 4. Both reactions proceed through nucleophilic addition of the OH group on the *N*-acylpyridinium carbonyl group and simultaneous proton abstraction from the nucleophilic OH group with the acetate anion.[11] Furthermore, the NH residue of the indolyl group (NH_{indole}) tightly coordinates with the acetate anion ($CO_{acetate}$) in the relatively stable TSs. Since the $NH_{indole}/CO_{acetate}$ hydrogen bond participates in both reactions, the energy difference between **TSm-cat1-1** and **TSd-cat1-1** should be attributed to other factors. The energetically favored **TSm-**

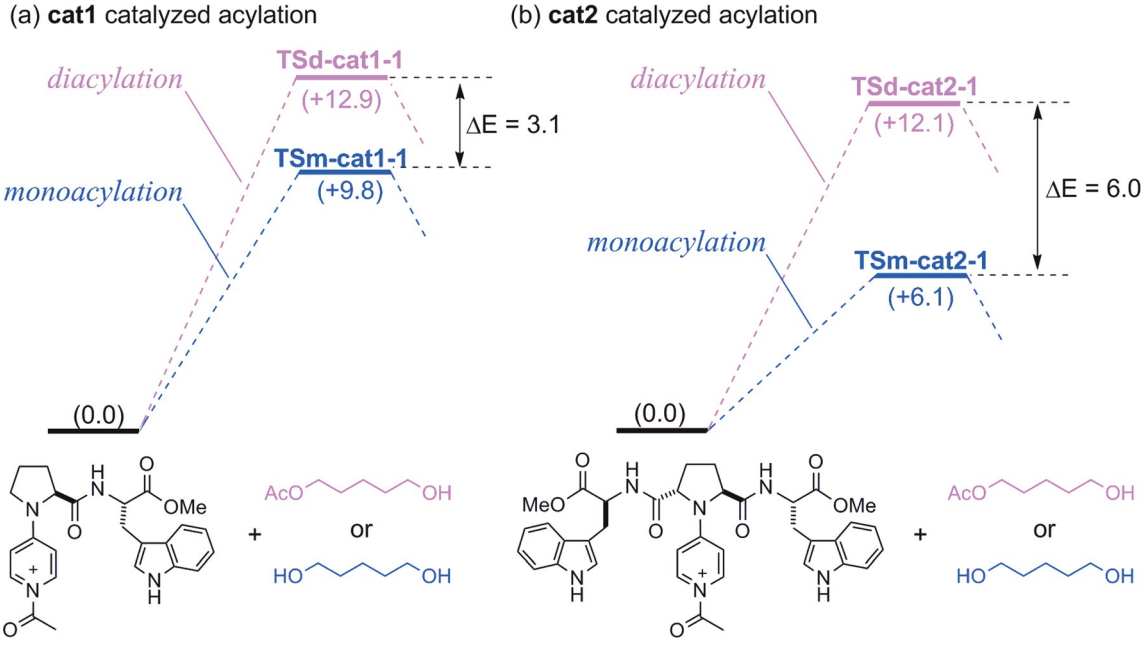

Figure 3. The relative Gibbs free energy differences (kcal mol^{-1}) between TSs of monoacylation (blue) and diacylation (purple) in (a) **cat1** and (b) **cat2** systems. The sum of acylated 4-PPY and the each substrates is set to zero.

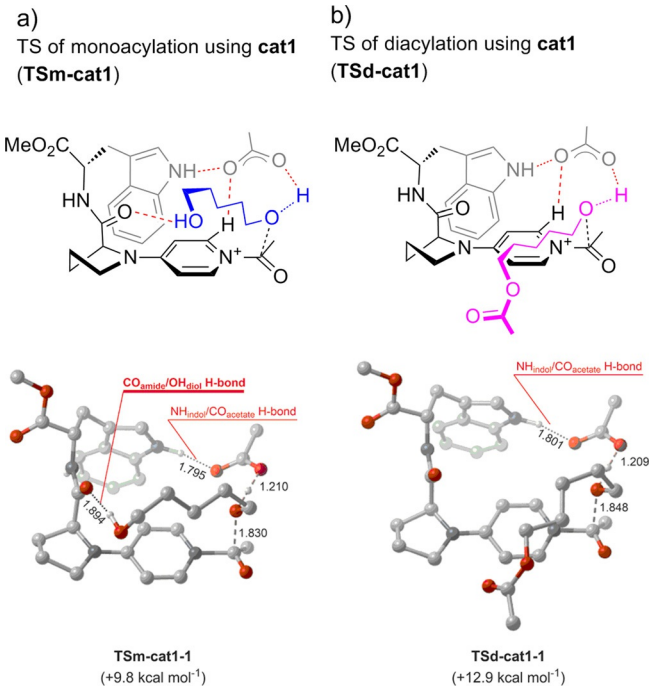

Figure 4. The 3D structures and the relative Gibbs free energies of (a) **TSm-cat1-1** and (b) **TSd-cat1-1**. Bond lengths are shown in Å. Hydrogen atoms of the CH groups are ignored.

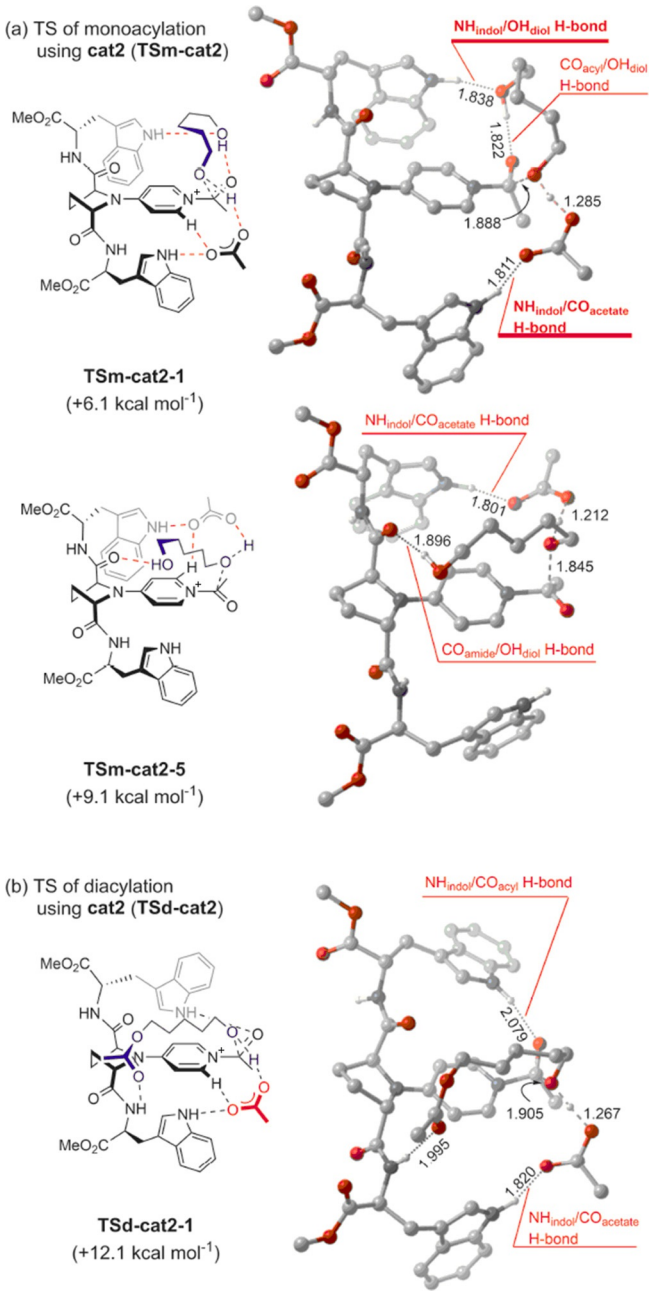

Figure 5. The 3D structures and the relative Gibbs free energies of (a) **TSm-cat2-1**, **TSm-cat2-5**, and (b) **TSd-cat2**. Bond lengths are shown in Å. Hydrogen atoms of the CH groups are ignored.

cat1-1 has the strong hydrogen bond between the amide carbonyl oxygen of **cat1** (CO$_{amide}$) and the remaining OH group of 1,5-diol **1** (OH$_{diol}$). The significantly strong CO$_{amide}$/OH$_{diol}$ hydrogen bond fixes the conformation of the substrate tightly and constructs the well-defined TS structure. The importance of the CO$_{amide}$/OH$_{diol}$ hydrogen bond has been also established in the highly *E*-selective PPY-catalyzed acylation of α,α-alkenediols.[12] In contrast, **TSd-cat1-1** does not have such an additional strong hydrogen bond but rather weak interactions between the Ac group and the C–H residue of the catalyst. **TSd-cat1-1** is therefore located at the higher energy level in comparison with **TSm-cat1-1**. The indicated importance of the CO$_{amide}$/OH$_{diol}$ hydrogen bond for stabilizarion of **TSm** is well consistent with the critical effect of the amide carbonyl group(s) at C-2 and/or C-5 of the pyrrolidine ring of the PPY catalysts on the chemoselective monoacylation of **1** shown in Table 2.

The experimental results indicates that two indolyl NH groups arranged in a C_2-symmetrical fashion in catalyst **4** play a key role in a significantly high level of molecular recognition for 1,5-diol **1** through TS stabilization. To clarify the origin of the molecular recognition ability of catalyst **4**, we continuously investigated TSs of monoacylation (**TSm-cat2**) and diacylation (**TSd-cat2**) in the **cat2** system (Figure 5). In a manner similar to the **cat1** system, the relatively stable TSs of both reactions have the strong NH$_{indole}$/CO$_{acetate}$ hydrogen bond. On the other hand, the two indolyl NH groups induce a significant change in the hydrogen bonding network in the most stable **TSm-cat2-1**. The OH$_{diol}$ residue coordinates with the negatively charged *N*-acylpyridinium carbonyl oxygen, increasing the Lewis basicity of the oxygen atom of OH$_{diol}$ to form the strong NH$_{indole}$/OH$_{diol}$ hydrogen bond. *The rational multiple hydrogen bonding network through two 3-indolyl groups, the acetate anion, and 1,5-pentanediol indeed stabilizes* ***TSm-cat2-1***. **TSm-cat2-5**

having a similar coordination mode with **TSm-cat1-1** is no longer the most stable **TSm-cat2**. This is because the second 3-indolyl group has no impact on the hydrogen bonding network in **TSm-cat2-5**. These results indicates that catalyst **4** (e.g., **cat2**) achieves the precise molecular recognition for 1,5-diol **1** through the quite different coordination mode from catalyst **7** (e.g., **cat1**). In **TSd-cat2-1**, the NH_{indole} residue directly coordinates with the negatively charged *N*-acylpyridinium carbonyl oxygen, forming the relatively weak hydrogen bond. The Ac group of the substrate does not coordinate with NH_{indole} residue but with the second amide NH residue. The two indolyl NH groups rarely contribute to the molecular recognition process of the substrate structure in the monoacylation.

Conclusions

The chemoselective monoacylation of 1,5-pentanediol (**1**) has been investigated with various C_1- and C_2-symmetrical PPY-catalysts. The amide carbonyl group(s) in the pyrrolidine ring of both C_1- and C_2-symmetrical catalysts was found to play a key role for the selective monoacylation. On the other hand, the indolyl NH group in the amide side chain of the catalyst was found to be critically important for further increasing the chemoselectivity of monoacylation only when the catalyst has a C_2-symmetrical structure. DFT calculations elucidate the origin of the precise molecular recognition for 1,5-diol and TS stabilization effect of C_2-symmetrical catalyst **4**. Two indolyl NH groups arranged in a C_2-symmetrical fashion in catalyst **4** cooperatively act to create the rational multiple hydrogen bonding network for significantly stabilizing the monoacylation TS of 1,5-diol **1**.

Experimental Section

General Information

All reactions were carried out in an argon atmosphere under anhydrous conditions. Anhydrous chloroform ($CHCl_3$) was purchased from Kanto Chemical Co., Inc. and stored over activated molecular sieves. Isobutyric anhydride and 2,4,6-collidine were distilled before use. Thin-layer chromatography (TLC) was performed on silica gel 60 F_{254} precoated plates (0.25 mm, Merck). Preparative TLC (PTLC) was carried out by using silica gel 60N F_{254} (0.5 mm, Merck). ^1H and ^{13}C NMR spectra were recorded on JEOL ECA-600 (600 and 150 MHz). Chemical shifts are reported relative to the solvent ($CHCl_3$: $\delta(^1H)=7.26$ ppm, $\delta(^{13}C)=77.0$ ppm, benzene-d_6: δ $(^1H)=7.16$ ppm) as reference. Data for ^1H NMR are reported as follows: chemical shift (δ ppm), integration, multiplicity (s = singlet, d = doublet, t = triplet, dd = double doublet, dt = double triplet, m = multiplet) and coupling constant (Hz). Data for proton-decoupled ^{13}C NMR are reported in terms of chemical shift. Infrared (IR) spectra were recorded on a JASCO FT-IR 4200 spectrometer and are reported in terms of frequency of absorption (cm^{-1}). High resolution mass spectra (HR-MS) were obtained using a Bruker Impact HD mass spectrometer. Specific rotations were measured with a JASCO P-2200 polarimeter, and are reported as follows: $[\alpha]_D^t$ [$c=10$ mg mL^{-1}, solvent, enantiomeric excess (*ee*)]. Melting points (mp) were measured with a Yanagimoto Micro Melting Point Apparatus PM-500.

General Procedure for the Acylation of 1,*n*-Diol (Table 2 and Table 3)

To a stirred solution of 1,*n*-diol (0.2 mmol, 1.0 equivalents), catalyst (5 mol%) and 2,4,6-collidine (1.5 equivalents) in $CHCl_3$ (2.9 mL, 0.07 M for 1,*n*-diol) at −60 °C was added cooled isobutyric anhydride (1.03 equivalents). After stirring at −60 °C for 24 h, the reaction mixture was quenched with MeOH (10 mL), and the solution was stirred for 10 min. Then the solvent was carefully evaporated. Yields of monoacylate, diacylate and recovered 1,*n*-diol were determined by NMR in $CDCl_3$ or benzene-d_6.

Procedure for the Competitive Acylation (Table 4)

To a stirred solution of 1,5-pentanediol (**1**) (0.16 mmol, 0.5 equivalents), 1,2-ethanediol (**13**) (0.16 mmol, 0.5 equivalents), catalyst (5 mol%) and 2,4,6-collidine (1.5 equivalents) in $CHCl_3$ (4.6 mL, 0.07 M for the total amount of diols) at −60 °C was added cooled isobutyric anhydride (1.03 equivalents). After stirring at −60 °C for 24 h, the reaction mixture was quenched with MeOH (16 mL), and the solution was stirred for 10 min. Then the solvent was carefully evaporated. Yields of monoacylates, diacylates and recovered diols were determined by NMR in $CDCl_3$ and benzene-d_6. Chemoselectivity of the acylation of 1,5-pentanediol (**1**) [$(k_{(\text{acylation of } \mathbf{1})}$] *versus* 1,2-ethanediol (**13**) [$k_{(\text{acylation of } \mathbf{13})}$] was determined according to the following equation:

$$\frac{k(\text{acylation of } \mathbf{1})}{k(\text{acylation of } \mathbf{13})} = \frac{\ln\left[(1-\text{conversion})\left(1-\frac{|(\mathbf{14}+\mathbf{15})-(\mathbf{2a}+\mathbf{3a})|}{\{(\mathbf{14}+\mathbf{15})+(\mathbf{2a}+\mathbf{3a})\}}\right)\right]}{\ln\left[(1-\text{conversion})\left(1+\frac{|(\mathbf{14}+\mathbf{15})-(\mathbf{2a}+\mathbf{3a})|}{\{(\mathbf{14}+\mathbf{15})+(\mathbf{2a}+\mathbf{3a})\}}\right)\right]}$$

The term $|(\mathbf{14}+\mathbf{15})-(\mathbf{2a}+\mathbf{3a})|$ indicates the absolute value of the difference between (**14**+**15**) and (**2a**+**3a**).

Conversion was calculated based on the total amount of the two diols.

Synthetic Procedures and Characterization Details of catalyst 8

To a solution of *N*-(4-pyridyl)-L-proline (23 mg, 0.1 mmol), 1-methyl-L-tryptophan octyl ester hydrochloride (55 mg, 0.15 mmol) in CH_2Cl_2 (1.1 mL) were added 1-ethyl-3-(3-dimethylaminopropyl)carbodiimide hydrochloride (EDCI) (29 mg, 0.15 mmol), 1-hydroxybenzotriazole (HOBt) (20 mg, 0.15 mmol) and *N*-methylmorpholine (44 μL, 0.4 mmol).

After stirring at room temperature for 12 h, the mixture was diluted with AcOEt and washed with saturated aqueous $NaHCO_3$ and brine, dried over Na_2SO_4, filtered, and concentrated under vacuum. The crude product was purified by preparative TLC (SiO_2, 1:19 MeOH/$CHCl_3$) to afford **8** as a white solid; yield: 50 mg (96%); mp 85–86 °C; $[\alpha]_D^{20}$: −103 (*c* 0.35, $CHCl_3$). ^{1}H NMR (600 MHz, $CDCl_3$): $\delta = 8.15$ (d, $J = 5.5$ Hz, 2H), 7.43 (d, $J = 7.9$ Hz, 1H), 7.26–7.21 (m, 2H), 7.11–7.08 (m, 1H), 6.68 (s, 1H), 6.44 (d, $J = 7.6$ Hz, 1H), 6.27–6.25 (m, 2H), 4.76–4.73 (m, 1H), 4.09 (dt, $J = 5.8$, 1.7 Hz, 2H), 3.98 (dd, $J = 9.1$, 1.7 Hz, 1H), 3.64 (s, 3H), 3.30 (dd, $J = 15.0$, 5.9 Hz, 1H), 3.23 (dd, $J = 15.0$, 5.9 Hz, 1H), 3.12–3.07 (m, 1H), 3.05–3.00 (m, 1H), 2.20–2.07 (m, 2H), 1.87–1.81 (m, 1H), 1.61–1.47 (m, 3H), 1.31–1.22 (m, 10H), 0.88 (t, $J = 6.8$ Hz, 3H). ^{13}C NMR (150 MHz, $CDCl_3$): $\delta =$ 172.0, 171.2, 151.7, 149.0, 136.7, 128.2, 127.2, 121.9, 119.3, 118.0, 109.6, 108.0, 107.7, 65.7, 63.0, 53.1, 48.3, 32.7, 31.8, 30.9, 29.2, 28.5, 26.4, 25.8, 23.4, 22.6, 14.1. IR (neat): $\nu =$ 3189, 2925, 1739, 1673, 1598, 1516, 1379, 1255, 1224, 999, 805, 743 cm^{-1}. HR-MS (ESI): $m/z = 505.3162$, calcd. for $C_{30}H_{40}N_4O_3$ $[M+H]^+$: 505.3173.

Acknowledgements

This work was financially supported by a Grant-in-Aid for Scientific Research on Innovative Areas "Advanced Molecular Transformations by Organocatalysts" and a Grant-in-Aid for Scientific Research (S) from MEXT. This work was also supported by a Grant-in-Aid for JSPS Fellows to A.I.

References

[1] K. Yoshida, T. Furuta, T. Kawabata, *Angew. Chem.* **2011**, *123*, 4990–4994; *Angew. Chem. Int. Ed.* **2011**, *50*, 4888–4892.

[2] a) S. Takahashi, T. Katagiri, K. Uneyama, *Chem. Commun.* **2005**, 3658–3660; b) M. Iwashita, K. Makide, T. Nonomura, Y. Misumi, Y. Otani, M. Ishida, R. Taguchi, M. Tsujimoto, J. Aoki, H. Arai, T. Ohwada, *J. Med. Chem.* **2009**, *52*, 5837–5863; c) H. E. Giesbrecht, B. J. Knight, N. R. Tanguileg, C. R. Emerson, P. R. Blakemore, *Synlett* **2010**, 374–378.

[3] a) A. B. Hajjar, P. F. Nicks, C. J. Knowles, *Biotechnol. Lett.* **1990**, *12*, 825–830; b) V. Framis, F. Camps, P. Clapés, *Tetrahedron Lett.* **2004**, *45*, 5031–5033.

[4] The difficulties in monoacylation of primary diols have also been indicated, see: C. A. Lewis, B. R. Sculimbrene, Y. Xu, S. J. Miller, *Org. Lett.* **2005**, *7*, 3021–3023.

[5] The ratio (**2a**/**3a**) in the acylation of **1** catalyzed by **4** depends slightly on the conditions. For example, **2a**/**3a** = 86: ≤1 under the conditions including **4** (10 mol%), $(i\text{-PrCO})_2O$ (1.03 equiv.), collidine (1.7 equiv.) in $CHCl_3$, at −60 °C for 24 h (data in Figure 1a in ref.[1]); **2a**/**3a** = 92:3 under the conditions including **4** (5 mol%), $(i\text{-PrCO})_2O$ (1.1 equiv.), collidine (1.5 equiv.) in $CHCl_3$, at −60 °C for 24 h (Table 1, entry 4); **2a**/**3a** = 80:3 under the conditions including **4** (5 mol%), $(i\text{-PrCO})_2O$ (1.03 equiv.), collidine (1.5 equiv.) in $CHCl_3$, at −60 °C for 24 h (Table 2, entry 1).

[6] DMAP-catalyzed acylation of **13** gave **14** and **15** in the ratio of 47/18, indicating the intrinsic higher reactivity of diol **13** than that of monool-monoacylate **14**.

[7] Monoacylate **14** formed from 1,2-diol **13** exists exclusively as an intramolecularly hydrogen-bonded cyclic conformer, which should be inert to acylation. On the other hand, monoacylate **2a** formed from 1,5-diol **1** exists exclusively as a linear conformer without a hydrogen bond, which should be reactive for acylation. Thus, selective monoacylation of 1,2-diol **13** was assumed to be achieved mainly in a substrate-controlled manner, whereas that of 1,5-diol **1** was done in a catalyst-controlled manner. For the relative stability differences between the cyclic and linear conformers of **2a** and **14**, see the Supporting Information.

[8] All calculations were carried out using *Gaussian 09* package. Computational details are shown in the Supporting information.

[9] The B3LYP functional tends to underestimate the hydrogen-bonding strength. As shown in our present study, however, B3LYP is adequate enough to describe the relative hydrogen bond energies. See: L. Rao, H. Ke, G. Fu, X. Xu, Y. Yan, *J. Chem. Theory Comput.* **2009**, *5*, 86–96, and references cited therein.

[10] Details of the preliminary screening of the rational TS models are described in the Supporting Information.

[11] Zipse reported a similar TS structure in the DMAP-catalyzed acylation of alcohols, see: S. Xu, I. Held, B. Kempf, H. Mayr, W. Steglich, H. Zipse, *Chem. Eur. J.* **2005**, *11*, 4751–4757.

[12] M. Yamanaka, U. Yoshida, M. Sato, T. Shigeta, K. Yoshida, T. Furuta, T. Kawabata, *J. Org. Chem.* **2015**, *80*, 3075–3082.

